

Journal of Mechanics of Materials and Structures

**RESISTANCE OF FLAT VAULTS TAKING THEIR
STEREOTOMY INTO ACCOUNT**

Mathias Fantin, Thierry Ciblac and Maurizio Brocato

Volume 13, No. 5

December 2018



RESISTANCE OF FLAT VAULTS TAKING THEIR STEREOTOMY INTO ACCOUNT

MATHIAS FANTIN, THIERRY CIBLAC AND MAURIZIO BROCATO

We study the structural performance of flat vaults, depending on the patterns of voussoirs. For this purpose, we propose three archetypes, derived from the 18th–19th century literature on stereotomy, with fit simplifications.

The ultimate structural answer of these models are evaluated, searching numerically for statically admissible loading conditions by means of an enhanced version of the thrust network analysis, assuming failure occurring by joints' opening, crushing or sliding, while voussoirs remain rigid.

The considered enhancements allow one to better capture the contact forces acting on the joints and to define consistently the safety factor of the structure. They are based on the introduction of additional partial branches in the thrust network that represent actions internal to the voussoirs and are essential to describe, at least in some cases, their rotational equilibrium, which is neglected by the standard analyses.

The three examples are compared by superposing their domains of statically admissible loadings, represented in terms of vertical uniformly distributed load vs. thrust. Our findings support but partly some of the conjectures presented in the 18th century and later literature, especially because of a plate effect that can be observed at the corners of these structures. They also allow us to classify flat vaults according to the local shape of the force network, as elliptical, parabolic or hyperbolic, thus opening to a new interpretation of their nature.

1. Introduction

A flat vault is a structural system, spanning horizontally with a reduced thickness, that withstands mainly vertical loads, normally its own weight plus additional dead and living loads, discharging them at its boundary by means of a vault effect, i.e., with a horizontal thrust. Flatness of the intrados is what characterises these structures with respect to standard (curved) vaults.

The vault effect we refer to is related to the fragmentation of the vault into voussoirs, with the joints having milder mechanical properties than the stones. Stereotomy is thus a paramount feature of these systems and our purpose here is to understand its role. Systems reaching supports in one piece, as monoliths, or stone-coffered ceilings whose span is covered by stone slabs, are not studied here.

Three bondings of flat vaults will be considered here, derived from historical examples presented in [Section 2](#), with parameters set in [Section 3](#), and their statically admissible ultimate structural performances compared by means of an enhanced version of the thrust network analysis.

The thrust network analysis [[O'Dwyer 1999](#); [Block and Ochsendorf 2007](#)] has been applied to produce form finding tools [[van Swinderen and Coenders 2009](#); [Rippmann et al. 2012](#)], and several advances and extensions have been published concerning the optimisation procedures [[Vouga et al. 2012](#); [Block and](#)

Keywords: vaults, stereotomy, limit analysis, thrust network analysis.

Lachauer 2014b] and the related variational formulations [Fraternali 2010; de Goes et al. 2013] that can be set up to define the parameters left otherwise undefined by the equilibrium equations. It has also been applied to some historical structures on gothic fan vaults [Block and Ochsendorf 2008], rose-windows, and thin-shelled spiral staircases [Block 2009; Block and Lachauer 2014a].

Flat vaults, as flat arches, are not distinguishable from each other by their form. Per se their strength depends on the pattern in which voussoirs are cut and laid. Hence the need arises for an analytical tool capable of gaining an insight into the vault's masonry bonding.

With this need in mind, the method proposed in Section 4 is based on a more-detailed-than-usual translation of the information on the structure into the arena where forces and strengths contend. While in the standard thrust network analysis voussoirs are related to mass-points (being the nodes of a network whose branches represent, but roughly, the connections between first neighbours), a refinement of this network is made here, subdividing voussoirs in such a way that the branches of the network are a more accurate representation of the forces exchanged across joints. This refinement has been already presented in [Ciblac and Fantin 2015; Fantin and Ciblac 2016; Fantin 2017] and is applied here to the cases at issue.

The numerical implementation of the method is briefly presented in Section 5 and the results are given in Section 6. It appears that the proposed refinement allows us to define more statically admissible states than the standard thrust network analysis does. Thanks to this result, the differences among the limit static interactions in the three studied cases can be displayed and discussed.

2. A historical survey on the stereotomy of flat vaults

Many options were available in the past for the stereotomy of flat vaults and technology opens even more today, but a taxonomy is needed for our purposes. A grouping proposed by Rondelet [1804] is handy, where cutting patterns are named with respect to their analogous in curved vaults, namely (see Figure 1, from left to right):

- (1) barrel vaults (*voûte en berceau* in [Rondelet 1804]);
- (2) pavillon vault (*voûte en arc de cloître*);
- (3) spherical vault (*coupole*);
- (4) groin vault (*voûte d'arêtes*).

Various examples of such flat vaults were built in France during the 16th, 17th, and 18th centuries [Pérouse de Montclos 1982], and many exist in other countries and from different ages (see [López Mozo 2003]).

The cases covered by this nomenclature share a common trait: loads decrease “monotonically” toward the boundary. The adverb can be qualitatively explained as follows: observing any voussoir, the sheaf of vertical planes cutting it through its centre contains one element across which shear forces are exchanged whose absolute value is minimal, the plane orthogonal to it in the same sheaf bearing the maximum absolute shear. When the minimal-valued shear is null, it is possible to sever all voussoirs along the then unique nonsheared plane, without changing the load descent.

If the pattern drawn by the intersection of the planes of maximum absolute shear with the plane of the vault is made of parallel lines, then the flat vault can be called unidirectional or parabolic (i.e., inheriting the properties of a barrel vault), as it is the case of item (1). Loading is discharged in one

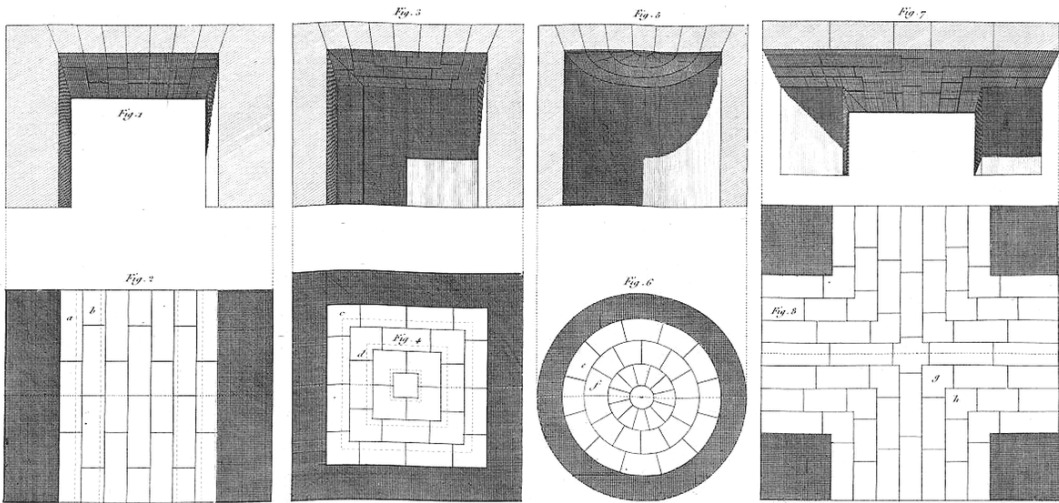


Figure 1. Flat vaults cutting pattern from [Rondelet 1804, Pl.XXXI; 1828, Pl.XXX].

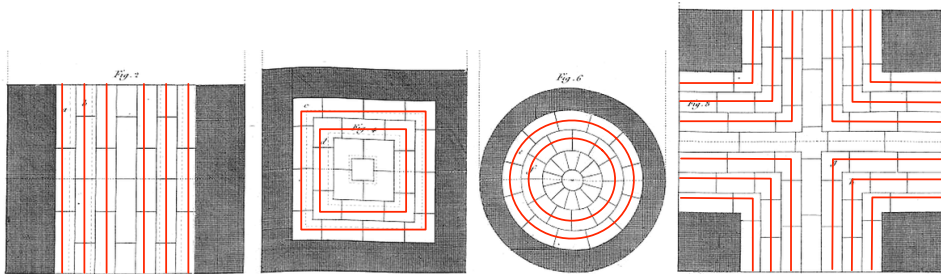


Figure 2. Patterns drawn by the maximum shear planes on the vaults of Figure 1: parallel lines correspond to a unidirectional or parabolic flat vault, concentric lines to a bidirectional or elliptical one.

direction (orthogonal to those lines) from one support to the other on two opposite sides of the vault, which necessarily covers a quadrilateral (possibly rectangular) surface, with nothing supporting the vault along the two other sides.

Otherwise, as concentric figures are found, one faces case (2) (concentric squares), (3) (circles), or (4) (cross-shaped figures). The vault can then be called bidirectional or elliptical (see Figure 2).

A third case can be considered, not in that list, with vaults that can be called hyperbolic: the above mentioned nonsheared plane is not unique, as two orthogonal planes partake of the same property at each voussoir. This dyad defines four quarters; two crossed by planes bearing positive shear forces, among which a plane of maximum shear exists, and two crossed by negative sheared planes, with one carrying a minimal shear.

These statements, presently calling upon intuition, will be made precise thanks to some of the developments presented herein. Three examples will be studied, representing the families of parabolic, elliptical, and hyperbolic flat vaults:

- (1) a “barrel” flat vault, akin to the first example on the left of [Figure 1](#);
- (2) a “pavillon” flat vault, akin to the second example from the left in the same figure;
- (3) an “Abeille” flat vault.

Abeille’s flat vaults are so named today after their inventor, Joseph Abeille, who lived in 18th century France. Though we have a first hint of their invention in [\[de Bélidor 1729\]](#)¹, we owe the earliest evidence of their geometry to Gallon [\[1735\]](#).

The vaults patented by Abeille in 1699 were, unlike any other existing example, made of one single type of voussoir: a trapezohedron, cut in such a way that the lower face is a rectangle, the upper a square, and the two central sections obtained through planes normal to the sides of the square are isosceles trapezia, one upside down with respect to the other. Thanks to this design, when voussoirs are properly assembled, the intrados form a continuous ceiling and the extrados form a floor with pyramidal gaps.

What makes Abeille’s vaults the paradigm of a whole family of new structures is their interlocking stereotomy. In the assembly, each voussoir has four first neighbours: two of them, at opposite sides in one direction, prevent it from moving downward, the other two from moving upward. Hence, when loaded, each sustains two neighbours and is sustained by the other two. It has then been noticed that these are, at the same time, “catenary” structures (or based on the principle of the inverted chain) and “levery” structures (or based on the principle of the lever [\[Brocato 2011; Brocato and Mondardini 2012\]](#)), as they partake of the nature of curved vaults and of nexorades [\[Baverel 2000; Baverel et al. 2000; Baverel and Nooshin 2007\]](#), possibly due to the influence on their author of a particular type of timber frame — later called Serlio’s floors [\[Émy 1837; Yeomans 1997\]](#) — existing much earlier as pictures by Villard De Honnecourt, Leonardo da Vinci, and Sebastiano Serlio indicate, and studied by his contemporary John Wallis (see [Figure 3](#), where two such frames are depicted, with reference to [\[Heyman 1995; Khandelwal et al. 2015\]](#)).

Already during his time, it was recognised that Abeille’s interlocking bond results in the possibility of building the system the other way around, with squares on top and pyramidal gaps above. Furthermore, alternative were proposed in the same session of the French Academy, without gaps, but using more complex cuts, by Sebastien Truchet (see [Figure 3](#)). Finally, and most importantly for our scope here, it was understood that these vaults ought to discharge loads equally on the four sides².

Even though the information on Abeille’s idea was not lost after it came out (19th century drawings of the assembly are conserved at the *Arts and Métiers* museum in Paris), only two flat vaults were built following it, in 18th and 19th century Spain (Lugo’s cathedral in 1769 and Casa de Mina de Limpia at Ponton de la Oliva in 1853 [\[Rabasa Díaz 1998; de Nichilo 2003; Uva 2003\]](#)). Nevertheless, a renewed attention has been devoted to this subject in the last decade and some stone structures built copying

¹“Mr Abeille Ingenieur du Canal de Picardie, a imaginé une construction de plate-Bande fort ingenieuse, la coupe des Clavaux en est singuliere & contribue beaucoup à diminuer la poussée que les piés-droits auroient à soutenir, j’en aurois volontiers fait la description si elle étoit venue à ma connoissance avant que les planches de ce second Livre fussent gravées.” — de Bélidor [\[1729, Livre II, p. 61\]](#).

²“Puisque les coupes des claveaux des *Voutes plates* [d’Abeille] sont tournées de quatre côtez alternativement, il est clair que ces voutes poussent aussi de quatre côtez, à la difference des *Platebandes*, qui ne poussent que de deux côtez; d’où il suit qu’elles font la moitié moins d’effort que les platebandes pour renverser leurs piedroits, & par consequent demandent moitié moins d’épaisseur de mur, ce qui est un avantage.” — Frézier [\[1738, Volume 2, p. 77\]](#).

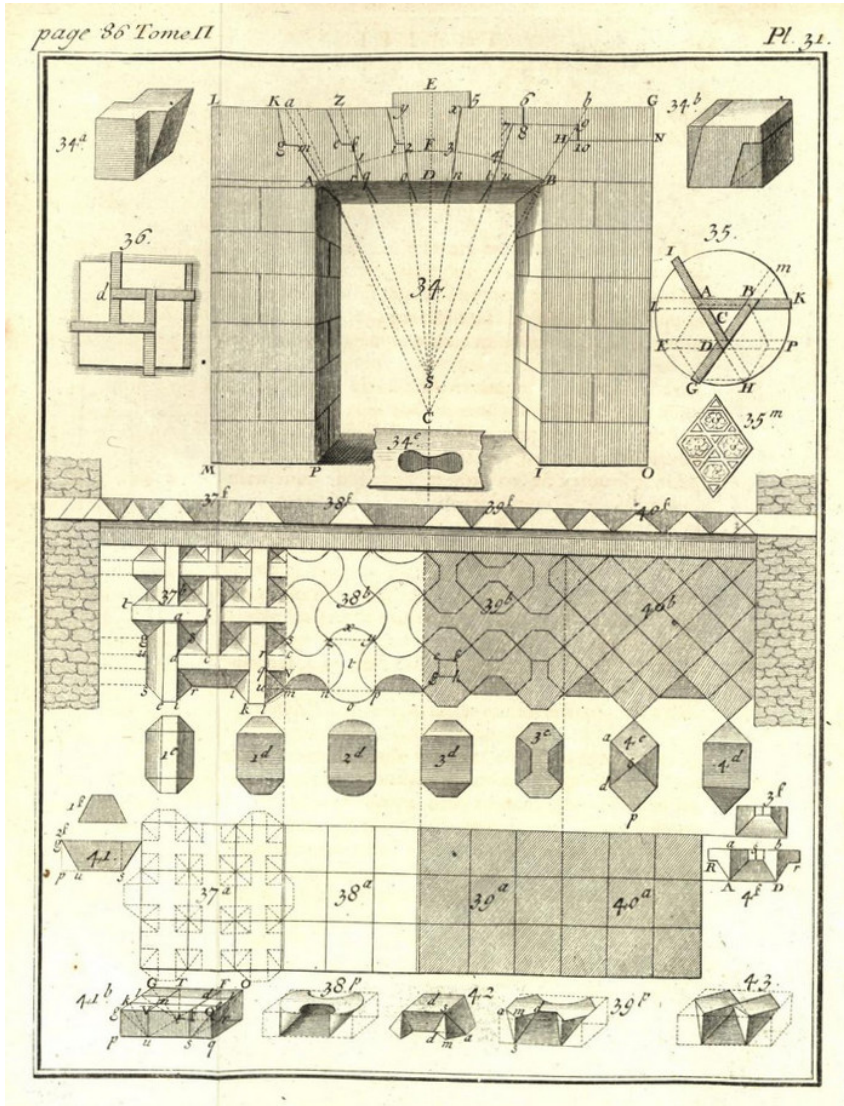


Figure 3. Alternative cuts proposed by Sebastien Truchet [Frézier 1738, Volume 2, Pl. 31].

or adapting Abeille’s interlocking principle [Etlin et al. 2008; Fallacara 2006; 2009; Sakarovitch 2006; Fleury 2009; 2010; Brocato and Mondardini 2010; 2012; 2015; Brocato et al. 2014; Mondardini 2015].

At Ponton de la Oliva, the dimensions are 3.10 m × 3.80 m × 0.21 m [Rabasa Díaz and López Mozo 2012]. Between 2003 and 2006, three vaults were built and loaded until failure at the Grands Ateliers de l’Isle d’Abeau (France), spanning square surfaces of side 2.52 m or 1.26 m, with thickness $\frac{1}{14}$ the span and joints inclined at 30° and 45° with respect to the vertical [Sakarovitch 2006; Fleury 2009; 2010].

At the same time, a vast literature has been produced on the subject of what has been — perhaps imprecisely — called “topologically interlocking materials” [Dyskin et al. 2001; 2003a; 2003b; Estrin et al. 2004; 2011; Khandelwal et al. 2012; 2015; Weizmann et al. 2016; Brocato 2018]. Abeille’s

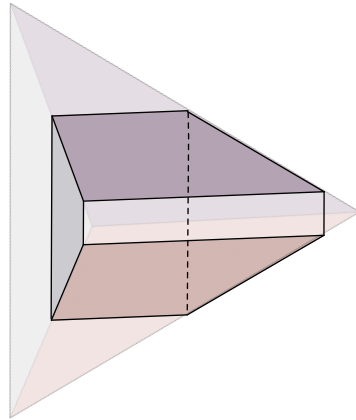


Figure 4. An example of how an Abeille’s voussoir can be obtained from a tetrahedron.



Figure 5. Vertical cut on the typical flat arch bonded according to the $\frac{1}{3}$ rule.

vaults appear then as a particular case, with interlocking blocks obtained by cutting a, possibly regular, tetrahedron with two parallel planes, one at half distance between any two nonconcurrent edges (see Figure 4).

3. Model settings

Our purpose is to perform a comparative limit analysis of the aforementioned three types of flat vaults: parabolic (or unidirectional), elliptical (or plainly bidirectional), and hyperbolic (or interlocking bidirectional). The geometries that we will define for this purpose are derived from some historical examples, but simplified to avoid unnecessary complexities.

The archetypal parabolic vault we consider here is an array of flat arches, closely disposed next to each other so that their lateral and vertical faces are in contact, but not otherwise bonded. Voussoirs are irregular polyhedra, whose upper and lower faces are squares, shifted in the direction of the span, so that two opposite faces rest vertically and the two others are suitably inclined. Their slope is defined following the so-called “1 on 3” rule of the French masons (see [Fantin 2017] for a thorough discussion on this and alternative rules in 18th and 19th century France), which means that it varies linearly between springers, where it takes the maximum absolute value of $\frac{1}{3}$, or an inclination on the vertical $\varphi = \arctan\left(\frac{1}{3}\right) = 18.4^\circ$ (see Figure 5).

It must be noticed that this disposition is not consistent with any known existing structure, because of the shift of courses that obviously appears there (see the rightmost drawing of Figure 1). As already mentioned in the previous paragraph, voussoirs can be ideally severed with planes containing the load descent path without changing this path; hence the geometry we use is statically consistent with what observable in practice (see Figure 6).

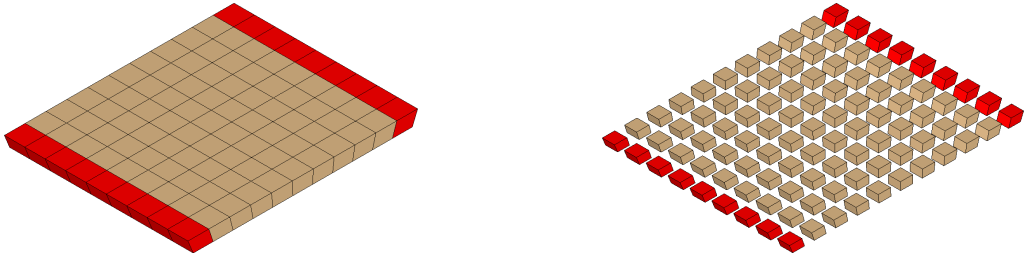


Figure 6. Archetype of a parabolic flat vault.

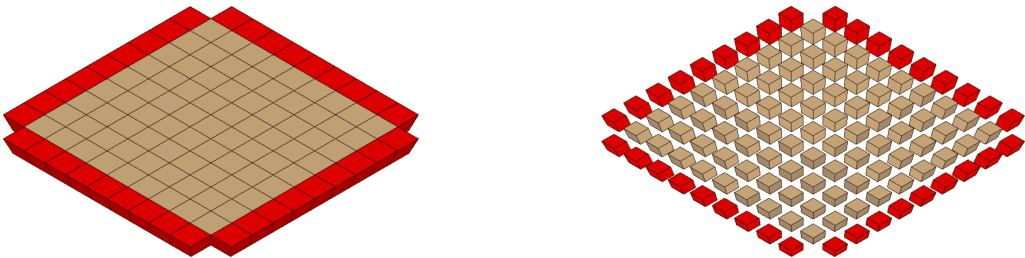


Figure 7. Archetype of an elliptical flat vault.

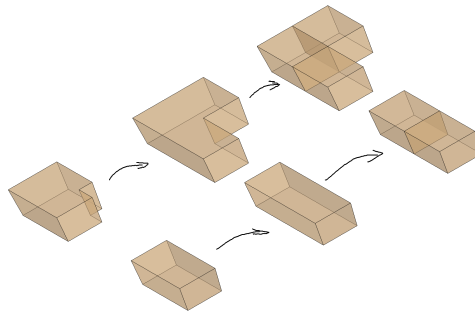


Figure 8. Simplification of the pattern of the elliptical flat vault adopted for numerical computations.

The model of elliptical flat vaults that we take into account is similar to the previous one, but now the square sides of the polyhedral voussoirs are shifted in a particular radial direction, so that all the other four faces are inclined. The inclination respects, again, the $\frac{1}{3}$ rule, but the progression is bidirectional, so that, if an array of flat arches is still observable in one direction, each arch leans on the next, proceeding from the centre to the springers, so that the same type of array can be observed in the orthogonal direction (see [Figure 7](#)).

As for parabolic vaults, in this case the model does not replicate the geometry of known examples, but remains statically representative of them because of the same principle concerning the severing of voussoirs along appropriate planes. Considering, for instance, the corner stones of the second structure from the left of [Figure 1](#), they are modelled here as any other piece of the assembly through the steps presented in [Figure 8](#), assuming that this simplification does not significantly affect results.

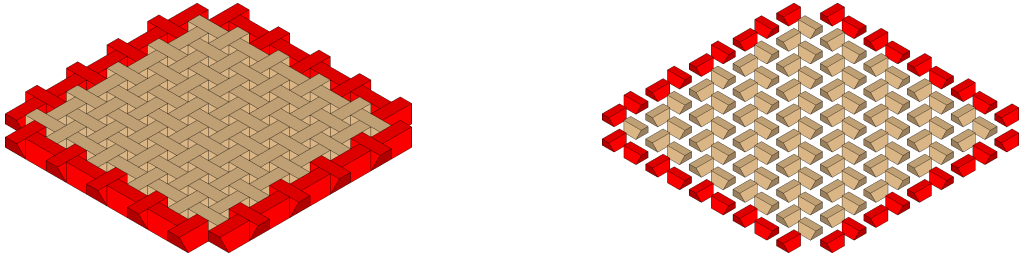


Figure 9. Archetype of a hyperbolic flat vault.

The hyperbolic flat vault archetype is made of voussoirs that can be described, in fair generality, by four parameters (see [Brocato and Mondardini 2015]), but, as the lower face of Abeille's voussoirs is meant to be a square, three suffice in the present case (when the lower face is not a square, then the gaps cross the vault through its whole thickness, or the cutting of the lateral sides is more complex than in Abeille's). The question is thus reduced to the same kind of information as in the previous cases, taking as independent parameters the side of the square, the thickness of the vault, and the angle of the joints with respect to the vertical. Differently than previously, here the angle is the same everywhere (as all voussoirs are equal) and we take the maximum angle defined by the $\frac{1}{3}$ rule, i.e., $\varphi = 18.4^\circ$. Notice that this choice is consistent with Gallon's written prescription [1735], which, as the author underlines, does not give the proportions that appear in his enclosed drawing.

As already mentioned, we are going to compare numerical results obtained for three models, the bonding of which has been presented above. Their overall geometry is the same: a square of 2.80 m, measured at mid-distance between the intrados and the extrados, with a thickness of 0.20 m (hence a ratio thickness on span of $\frac{1}{14}$). All structures are composed of $9 \times 9 = 81$ voussoirs. The considered mechanical properties are

- density (1658 kg/m^3),
- compression strength (10 MPa), and
- friction coefficient (0.7).

The loading applied for the analyses are a vertical force, uniformly distributed on the horizontal surface of the vault, and a set of forces acting independently on each of the springers of the vault. The latter have a vertical component, equilibrating the distributed force, but otherwise freely set, and a free horizontal component, or thrust, which is assumed to be orthogonal to the perimeter of the vault.

The purpose of the limit analysis is to determine a domain where the loading respects at the same time the equilibrium conditions and all safety criteria related, at the joints, to the limited compression strength, the null tension strength, and the Coulomb's friction.

The variables used to describe such domains of statically admissible loads in two dimensions are the intensity of the resultant of the vertical forces W and the intensity of the resultant of the horizontal thrusts at one side of the perimeter of the vault, say, in the x direction, $\sum H_x$.

Notice that while the parabolic vault springs from two sides only, the elliptical vault has a diagonal symmetry and thus acts equally on all sides, and the hyperbolic vault is chiral, so that it can be assumed

that the sums of the normal components of its actions along two consecutive sides of the perimeter are equal.

To handle dimensionless variables, the above mentioned forces are considered per unit weight of the vaults, so that the domains will be plotted in the W/W_0 vs. $\sum H_x/W_0$ plane, with W_0 being the total weight of the structure. Due to the gaps left by the bonding, Abeille's vault is lighter than the two others and we have

- parabolic and elliptical vault: $W_0 = 26.00$ kN;
- hyperbolic vault: $W_0 = 23.19$ kN.

4. Computational method

The planned comparisons will be carried on in the framework of limit analysis. The reason is two-fold: first, this analysis gives a hint on the ultimate structural performance requiring the least possible nongeometrical information; second, it addresses mechanical concepts (related to the onset of failure) that are, as much as possible, close to those that were used in the 18th and 19th centuries, when the debate on flat vaults flourished.

Within the broad field of limit analysis, an offspring of the force network method as first published by O'Dwyer [1999] is used here. This method generalises to three dimensions the funicular polygons constructed in two dimensional graphic statics. In short, it consists in finding the shape given by gravity to a net loaded by known weights at its nodes and respecting appropriate conditions at its boundaries, assuming the horizontal projection of the net is fixed, so that only the vertical position of the nodes at equilibrium is unknown. The solution of this problem defines both the shape of the net and the internal forces in the fabric depending on as many parameters as the assumption that the former does not depend on the intensity of the forces implies. If directly applicable to inextensible tensile nets (which generalise catenaries), the problem can be also translated to masonry vaults, where it helps define a network that generalised the concept of the inverted catenary (or the inverted funicular of a dead load). This method was extended by [Block and Ochsendorf 2007], with the use of reciprocal figures, under the name of thrust network analysis.

Consider a mass network, i.e., the network built on a given vault, with nodes corresponding to the centres of gravity of the voussoirs and branches corresponding to the interfaces between them; the thrust network analysis workflow is as follows:

- (1) Vertical forces are assigned at the nodes, corresponding to the weights of the voussoirs.
- (2) A cost function is defined, depending on the vertical coordinates of the nodes.
- (3) The geometry of the network projected on the horizontal plane is assigned.
- (4) The vertical positions of the boundary nodes are assigned (fit for the cost function); they are chosen among the parameters that will be left undetermined by the equilibrium problem and become the degrees of freedom of the optimisation problem.
- (5) A given number of force parameters is assigned, depending on the static indeterminacy of the system (usually corresponding to the thrusts along the branches of the network); they join the previous ones in the list of the degrees of freedom of the optimisation problem.

- (6) The set of internal forces verifying the self equilibrium of the network when projected in the horizontal plane is determined on the basis of the information provided in steps (3)–(5) (notice that, as only vertical loads will be applied, they are not considered at this step).
- (7) The vertical coordinates of the nodes and the internal forces in the branches are determined respecting the vertical equilibrium of the system under the load given at step (1) and the finding of step (6).
- (8) The value of the cost function of step (2) is computed.
- (9) Coming iteratively back to step (4), an optimisation procedure is run to define the best set of degrees of freedom based on the cost function defined at step (2).

When used as a limit analysis tool, this method is generally used to find, among all networks generated by the parameters, those whose nodes fall within the limits of the masonry structure. Notwithstanding the recurrence of the idea that this result can be directly related to safety (see [O’Dwyer 1999; Block and Ochsendorf 2008; Block 2009; Block and Lachauer 2014a; 2014b]), a digression is needed here.

In a vault made of voussoirs, failure may occur by opening joints. The relevant information is then the set of centres of pressure, i.e., the points where the resultant of the contact stresses intersects the plane of the joint. The safe theorem expressed by Heyman [1995] helps conclude that the vault is stable — under the hypotheses that the joints offer no tensile strength and infinite compressive strength, and suffer no sliding — if all centres of pressure fall within the convex hull of the corresponding contact surface (and fall strictly within it in a sufficient number of fit sequences to avoid potential failure).

Any stability condition expressed in terms of positions of the nodes is then to be understood as an approximation of the one deduced from the safe theorem, which concerns the positions of centres of pressure, even though the two sets are correlated. Clearly, in the limit of infinitesimal voussoirs, i.e., when both the distance between subsequent joints and the thickness of the vault tend to zero, the network of nodes coincides with that of centres of pressure, but if any of the two characteristic lengths quoted above are finite, the two pieces of information are distinct. This difference can be deemed negligible when the method is applied to form finding for design purposes, as then the voussoir’s geometry is defined after the thrust network. On the contrary, it is not so in at least one of the cases at issue, namely in hyperbolic flat vaults.

To tackle problems where the limit of infinitesimal voussoirs can’t be accepted and enhance the thrust network method as a tool to study existing masonry structures, the first two authors have analysed some historical methods for vault calculation and proposed the introduction of new equilibrium states among those available for the net by considering additional partial branches as described below [Ciblac and Fantin 2015; Fantin and Ciblac 2016].

The thrust network analysis is based on the hypothesis that all forces applied to one voussoir converge into one point, taken as a node of the thrust network. This is a sufficient but not a necessary condition to ensure moment equilibrium of the voussoir. Considering a single block subject to four forces and its own weight, four different equilibrium cases can be given, as shown in Figure 10. Only the case (a) respects the intersection hypothesis, and can thus be produced by a thrust network analysis, as in cases (b), (c), and (d), although force and moment equilibrium are fulfilled, forces intersect in two points, or do not intersect at all.

Notice that in case (b), the intersections of the forces take place in two distinct nodes, instead of one, but the horizontal projections of these nodes are identical. This configuration can be obtained using the

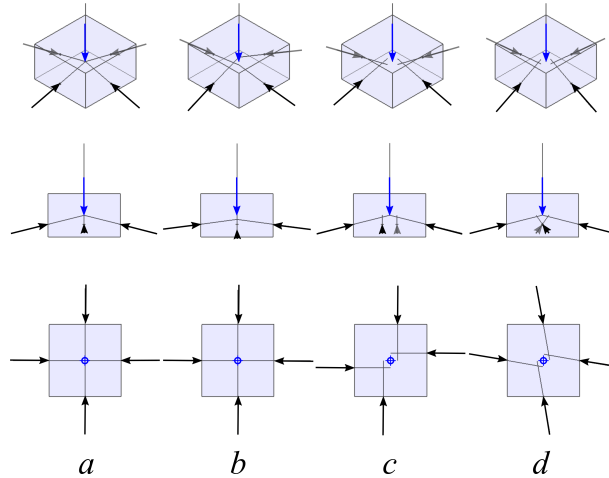


Figure 10. Equilibrium cases: (a) concurrent forces and (b-d) nonconcurrent forces.

particular mass network refinement proposed by Fantin and Ciblac [2016]. For this purpose, instead of relating each voussoir to one and only one node in the mass network, let us divide it into two smaller units and create correspondingly two nodes in the network, with their respective masses. The two nodes are joined by a new branch, which we call the “additional partial branch”, that is related to the internal force across the surface splitting the voussoir. The other branches of the network, which normally connect any two adjacent nodes and can be called “standard thrusting branches”, are not necessarily doubled in this process, as they are defined in such a way that each carries a relevant piece of information on a joint between voussoirs (e.g., one branch per joint).

Let us focus on the case when all additional partial branches are vertical (i.e., voussoirs are ideally split by one horizontal cut; notice that it is possible, though not needed here, to remove this assumption [Fantin and Ciblac 2016]). Then, the horizontal equilibrium of step (6) in the workflow above, not taking into account the forces in the additional partial branches, leaves them undetermined. Consequently, neither can the vertical equilibrium of step (7) be used to compute them. Hence, these forces must be included in the list of the degrees of freedom in the optimisation problem. Figure 11 illustrates the case when the mass refinement splits one node into two, belonging to the same vertical line, which allows one to consider an equilibrium similar to case (b) of Figure 10, but not cases (c) and (d).

When it comes to the optimisation procedure, the method of [Ciblac and Fantin 2015; Fantin and Ciblac 2016] introduces another variant to the thrust network analysis: the cost function is not built uniquely on the vertical coordinates of the nodes, as it takes into account the intersections of each of the standard thrusting branches with the surface of the corresponding joint. This is an important advantage, as the processed information is now consistent with the safety criteria of vaults for joint opening or sliding, even if, to obtain it, a much larger problem than the standard must have been posed by including the forces along the additional partial branches among the degrees of freedom of the system.

In particular, it is handy using as the cost function the global coefficient of safety of the structure, defined as the Euclidean distance between the quoted intersection and the boundary of the joint, which requires some additional computational stratagem to be quickly evaluated.

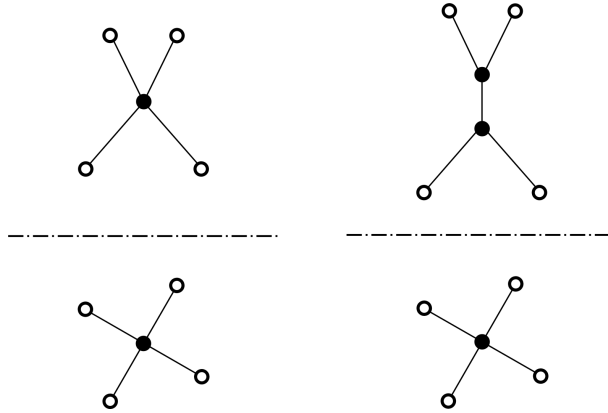


Figure 11. Front view (top) and horizontal projection (bottom) of a four-valent node before (left) and after (right) mass network refinement.

5. Numerical implementation

A numerical application of the described extension of the thrust network analysis, named Manacoh, was implemented in a Microsoft Excel worksheet with Visual Basic developments. Manacoh and its tutorials are freely available in a dedicated web site (<http://bestrema.fr/manacoh/>). It builds the geometry for parametric preset examples (specific geometries can also be loaded), solves the equilibrium equations, and offers the possibility to explore various equilibrium solutions through optimisation strategies derived from historical examples and including the techniques presented in this paper.

Because the computing capacity of Manacoh is relatively limited by the use of a general public environment, some numerical stratagems have been used to reduce the duration of computations. The various types of degrees of freedom (the horizontal forces in the standard thrusting branches, the vertical position of the boundary nodes, and the vertical forces in the additional partial branches) usually exhibit some regularity when at the optimum solution, provided that the structure studied has a regular geometry. This potential regularity is exploited by Manacoh, calling upon Lagrange polynomials to interpolate the degrees of freedom and thus lessen the number of free parameters in the optimisation process.

A second numerical scheme to make computations faster is the smoothing of the cost function by the following type of approximation: given any real function $d(x)$,

$$x : \min_x \|d(x)\| \approx x : \min_x (d(x)^{-p})^{-1/p} \quad \text{for } p \geq p_0 > 0;$$

p_0 being large enough for the approximation to be acceptable.

The type and number of degrees of freedom in the parabolic case, not introducing additional partial branches with respect to the standard thrust network analysis, are

- (A) 9 horizontal thrusts, becoming 1 by translational invariance;
 - (B) 18 vertical coordinates of the boundary nodes, becoming 1 by translational invariance and symmetry;
- when including partial branches, this case requires the additional

(C) 81 internal forces in the vertical partial branches, becoming 5 by translational invariance and symmetry.

In the elliptical cases, not introducing additional partial branches,

(A) 18 horizontal thrusts, becoming 5 by symmetry;

(B) 36 vertical coordinates of the boundary nodes, becoming 5 by symmetry;

when including partial branches, add

(C) 81 internal forces in the vertical partial branches, becoming 10 by symmetry;

thus rising the size of the problem to a minimal number of 20 degrees of freedom.

To lighten the optimisation problem in the second case, the (A) and (B) parameters were separately interpolated by a Lagrange polynomial of degree $k = 0, 2, \text{ or } 9$ ($k = 0$ means that a uniform thrust and an equal vertical position of the boundary nodes are considered, $k = 9$ means no interpolation).

The Abeille vault possesses less symmetries than the previous ones and it is not possible to analyse it by the standard method without partial branches. The total number of degrees of freedom is in this case 45, divided as follows:

(A) 18 horizontal thrusts, becoming 10 by symmetry;

(B) 36 vertical coordinates of the boundary nodes, becoming 10 by symmetry;

(C) 81 internal forces in the vertical partial branches, becoming 25 by symmetry.

Performing calculations with a smaller Abeille vault (5×5 voussoirs) it has been observed that the forces in the partial branches of the optimum solution depend approximately linearly on the distance from the centre of the vault. Hence, in addition to the interpolation by Lagrange polynomials of degree k of the (A) and (B) parameters, an approximation of the (C) parameters with polynomials of degree $r = 2$ in the quoted distance has been implemented to reduce the optimisation problem.

In any case, the domains of statically admissible loads were computed taking into account the intersections of the standard thrusting branches with the joints, not the positions of the nodes of the network. Processing this information it is also possible to take friction into account, by checking that the slope of the branch on the surface of the joint is below the limit of Coulomb's friction coefficient.

6. Results on the statically admissible loadings

Results obtained for the parabolic and elliptical vault are plotted in Figure 12. From the point of view of the method used for the analysis, they show that the introduction of partial branches improves the result, as it helps find a larger domain of statically admissible loadings (orange plots), especially if the forces in all partial branches are taken into account ($F_v \neq 0$, light orange case in the plot).

If the forces in all partial branches are taken as null ($F_v = 0$, dark orange case in the plot), the thrusting branches along the x and the y axis are totally independent from each other. This type of solution cannot be attained with a standard thrust network analysis without partial branches. The computed domain is, as expected, very close to an affine transformation of the domain of the parabolic vault doubling the vertical extent (compare the dark orange and grey plots in Figure 12). This result is a better approximation than the best obtained without partial branches (light blue plot) at least in the range of mid to high thrusts and

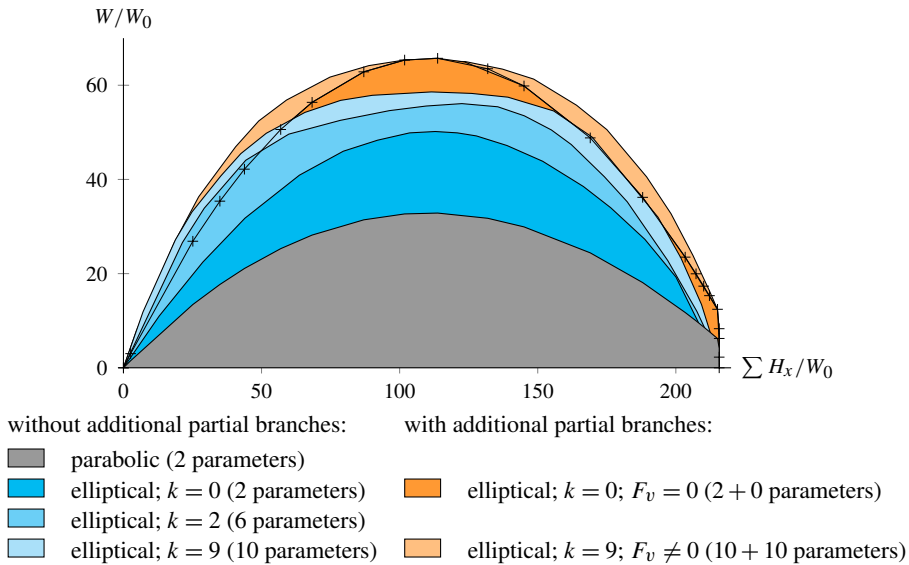


Figure 12. Domains of the statically admissible loadings in the a-dimensional thrust vs. weight plane, for parabolic and elliptical flat vaults. The results obtained by the refined method, including partial branches, displayed in orange, give a better approximation of the real domain.

it has been obtained with only two parameters, instead of the ten required by the competing unrefined network.

From the point of view of the numerical tools, even if the interpolation with Lagrange polynomials reduces — more than expected — the size of the domain, it is useful for finding a good starting point, which is crucial for optimisation. To test this advantage, we have started an optimisation with $k = 0$, then use the found optimal solution to start a new optimisation process with $k = 2$ and finally go from this result to the one with $k = 9$. This process was found to be much more time efficient than optimising directly without interpolation.

Finally, from the point of view of the structural comparison, we observe that the domain of statically admissible loading of the elliptical flat vault is notably larger than the domain of the parabolic one, with the elliptical vault performing better than the sum of two (orthogonal) parabolic ones (see the difference between the grey and light orange plots in Figure 12; in the same figure, the boundary of the domain obtained doubling the height of the grey plot is a line marked by +).

Examples of the shape of the related thrust networks are given in Figures 13 and 14. It can be observed that the addition of partial branches allows the lines of thrust to gain more inclination where the release of a larger shear is needed, while the orthogonal lines may come closer to the shape of an ideal catenary. This effect is particularly important in the vicinity of the boundary, where an equivalent plate would experience negative bending moments and withstand Kirchhoff shear forces pointing downward at the corners.

Results concerning the hyperbolic, or Abeille’s, vault are shown in Figure 15, superposed to the largest domains obtained for the other cases.

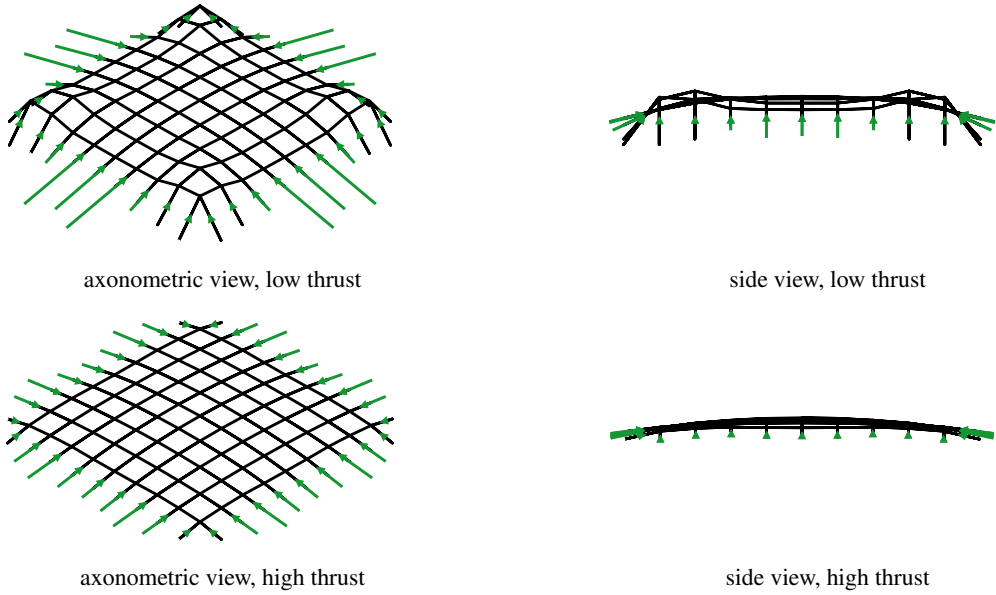


Figure 13. Axonometric view (left) and side view (right) of thrust networks without additional branches for the elliptical flat vault, computed for $k = 9$, under low thrust (above) and high thrust (below).

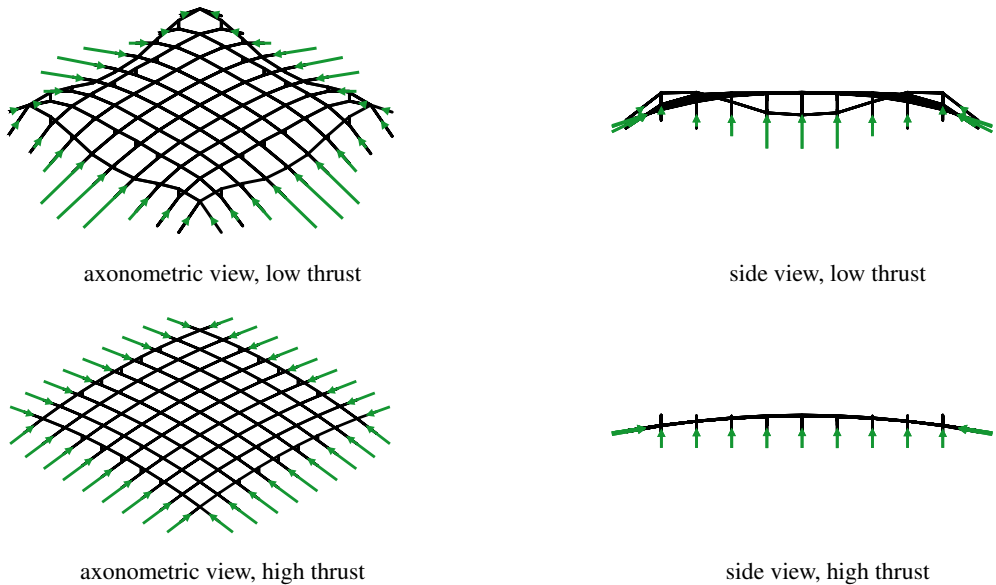


Figure 14. Axonometric view (left) and side view (right) of thrust networks with additional partial branches for the elliptical flat vault, computed for $k = 9$ and $F_v \neq 0$, under low thrust (above) and high thrust (below).

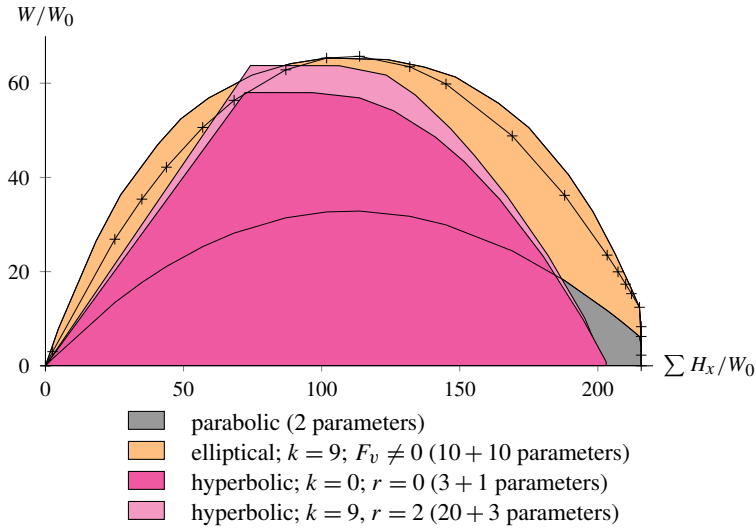


Figure 15. Domains of the statically admissible positive loadings for Abeille’s vault, compared to those of the parabolic and elliptical vault. Notice that Abeille’s vault admits negative loadings.

Notice that the boundaries of the domains displayed for the parabolic and the elliptical vault do not include parts depending on the selected value of the friction coefficient: failure of these vaults occurs always by opening of the joints. This is not the case of Abeille’s vault, where the friction criterion controls the minimum thrust (an infinite resistance to friction entailing the possibility of supporting vertical loads with no thrust) and thus the domains of statically admissible loadings are limited from the side of small thrusts by a straight line corresponding to the limit of failure by sliding.

Still from the point of view of the structural comparison of the three systems, it can be observed that the domain of the hyperbolic one is smaller than that of the two others for high thrust, due to the smaller size of the joints in the former. The hyperbolic vault performs otherwise better than the parabolic one and is quite close to the elliptical vault only for middle thrusts, being less resistant than the latter in the range of low thrusts.

Finally, it must be observed that only the part of the domain of Abeille’s vault including positive loads is displayed in Figure 15; this vault can actually withstand forces in the opposite direction within the same or very close limits, which is not possible for the two others.

Observing Figure 14, the adjective elliptical designating this type of vault can be explained, at least within the accuracy limits of the thrust network image of the internal actions. Let us call $z_{ij}^{(x)}$ and $z_{ij}^{(y)}$ the vertical coordinates of the two nodes of the network representing one voussoir (i.e., joined by a vertical, additional partial branch), assume i counting nodes having the same y coordinate and j having the same x and the exponent in $z_{ij}^{(x)}$ and $z_{ij}^{(y)}$ denote the direction along which the node is connected to its neighbours by a standard thrusting branch.

Let us define, at any point ij ,

$$\kappa_{ij}^{(x)} = z_{i-1j}^{(x)} - 2z_{ij}^{(x)} + z_{i+1j}^{(x)}; \quad \kappa_{ij}^{(y)} = z_{ij-1}^{(y)} - 2z_{ij}^{(y)} + z_{ij+1}^{(y)}.$$

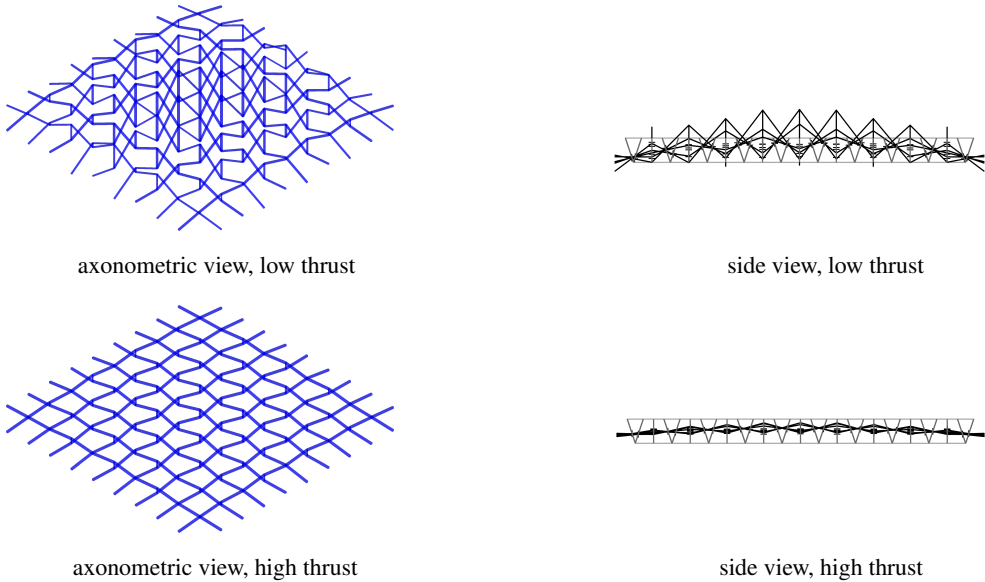


Figure 16. Axonometric view (left) and side view (right) of thrust networks with additional partial branches for the hyperbolic flat vault, computed for $k = 9$ and $r = 2$, under low thrust (above) and high thrust (below).

Any two nodes of the network representing one voussoir are in equilibrium under the weight of the voussoir and the four forces acting along the standard thrusting branches. With the exception of some of the boundary nodes, these four internal forces point upward; it is

$$\kappa_{ij}^{(x)} \kappa_{ij}^{(y)} > 0. \tag{6-1}$$

If we denote by $v_{ij/hj}$ the vertical component of the force carried by the branch joining the ij node with the hj node and $v_{ij/ik}$ that joining the ij with ik , the equality of the signs of the thrusts in the x and y direction entail

$$\text{sgn}((v_{ij/i-1j} - v_{ij/i+1j})(v_{ij/ij-1} - v_{ij/ij+1})) = \text{sgn}(\kappa_{ij}^{(x)} \kappa_{ij}^{(y)});$$

which means that the net contributions of the branches converging on the ij node in the two directions point upward when (6-1) is true (both opposed to the external force).

Observing Figure 16, on the contrary, we find

$$\kappa_{ij}^{(x)} \kappa_{ij}^{(y)} < 0, \tag{6-2}$$

with two branches pushing upward and two downward. Finally, even if not graphically presented here, the case of parabolic vaults is evidently one where

$$\kappa_{ij}^{(x)} \kappa_{ij}^{(y)} = 0, \tag{6-3}$$

and one of the two couples of branches is inactive.

Let us imagine the surface that has, locally at ij , $\kappa_{ij}^{(x)}$ and $\kappa_{ij}^{(y)}$ as curvatures and x and y as principal directions of curvature. This surface has there a Dupin's indicatrix that is an ellipse if $\kappa_{ij}^{(x)} \kappa_{ij}^{(y)} > 0$,

a parabola if $\kappa_{ij}^{(x)} \kappa_{ij}^{(y)} = 0$ and a hyperbola if $\kappa_{ij}^{(x)} \kappa_{ij}^{(y)} < 0$; correspondingly, ij is currently named an elliptical, parabolic, or hyperbolic point of the surface.

By analogy with this nomenclature, we named elliptical the flat vault having a thrust network whose “analogous” surfaces have (almost everywhere) elliptical points, parabolic the vault whose limit surfaces have a.e. parabolic points, and hyperbolic those whose limit surfaces have a.e. hyperbolic points. Equations (6-1), (6-2), and (6-3) disambiguate the attribution.

Statically, this characteristic entails that some branches push upward, some downward (as explained before), hence the image presented in Section 2 of a “monotonic” load descent in parabolic and elliptical vaults, with the maximally sheared plane corresponding to the maximum force acting along a standard thrusting branch and a minimally sheared plane corresponding to the minimal force along such a branch (clearly, the case where max and min coincide being possible).

In the case of hyperbolic flat vaults, the max and min shear have opposite sign, hence the image of a local division of the voussoir in quarters, with alternating shears.

7. Conclusion

Three model flat vaults, derived from historical examples, have been compared on the basis of their statically admissible loadings, using an enhanced version of the thrust network analysis:

- (1) a unidirectional vault, designed following the pattern of a “barrel” vault and named here parabolic;
- (2) a plainly bidirectional vault, having the pattern of a “pavillon” vault and named here elliptical;
- (3) an interlocking bidirectional vault, made according to Abeille’s system, which we named hyperbolic.

The work presented here lead to the conclusion that an enhancement of the thrust network analysis, taking more precisely into account the rotational equilibrium of voussoirs, is necessary to capture a wider domain of statically admissible loadings and, in one case, to be able to describe the system at all.

Computations were performed on a Microsoft Excel-based application, named Manacoh, developed by the first and second authors and publicly accessible on the internet. Some numerical expedients, called here to circumvent limitations arising from the use of a general public environment, can prove useful to handle large systems within more powerful numerical implementations. In particular, Lagrange polynomials can reduce the computational effort when used to interpolate iteratively the degrees of freedom of the optimisation procedure inherent in the thrust network analysis.

The comparison of the three archetypes shows that the bonding of voussoirs plays — as expected — a fundamental role in their stability, with system (1) having the best performances under vertical descending loadings and system (2), the resistance of which is quite close to that of the former, being also capable of withstanding ascending loadings.

Observing the thrust networks obtained in the different cases at the onset of failure, it is possible to gain an insight on the mechanical behaviour of flat vaults (at least if the shift from the limit is allowed). If parabolic flat vaults are plainly catenary structures (with parallel discharge arches bridging across supports), the elliptical ones are not exactly so and hyperbolic even less.

Elliptical vaults mimic the behaviour of continuous plates and thus the rotational equilibrium of their voussoirs plays an important role when close to the corners. In these areas the enhanced thrust network

displays the superposition of two inverted catenary structures, but not the existence of a single inverted “catenary net”, which can be observed elsewhere in the structure.

Hyperbolic flat vaults do not show at all the formation of such a single net, so that they can barely be considered catenary structures. Their thrust networks are wavy, not as a single net could do, but as a weaving fabric. Each voussoir, bearing shear forces of alternating sign at quarters of the horizontal projection, works both as a lever and as the link of an inverted chain, which confirms the idea that these are partly catenary and partly “levery” structures, if the neologism is accepted.

Acknowledgements

The results presented in this paper have been obtained during Mr. Fantin’s doctorate. The authors thank for his help on numerical methods Marco Czarnecki, Institut de Mathématiques et Modélisation de Montpellier, UMR 5030 CNRS, Université Montpellier 2, France.

References

- [Baverel 2000] O. L. S. Baverel, *Nexorades: a family of interwoven space structures*, Ph.D. thesis, University of Surrey, 2000, <https://tinyurl.com/bavnex>.
- [Baverel and Nooshin 2007] O. Baverel and H. Nooshin, “Nexorades based on regular polyhedra”, *Nexus Netw. J.* **9**:2 (2007), 281–298.
- [Baverel et al. 2000] O. Baverel, H. Nooshin, Y. Kuroiwa, and G. A. R. Parke, “Nexorades”, *Int. J. Space Struct.* **15**:2 (2000), 155–159.
- [de Bélidor 1729] B. F. de Bélidor, *La science des ingénieurs dans la conduite des travaux de fortification et d’architecture civile*, Jombert, Paris, 1729.
- [Block 2009] P. C. V. Block, *Thrust network analysis: exploring three-dimensional equilibrium*, Ph.D. thesis, Massachusetts Institute of Technology, 2009, <https://tinyurl.com/phdbloc>.
- [Block and Lachauer 2014a] P. Block and L. Lachauer, “Three-dimensional (3D) equilibrium analysis of Gothic masonry vaults”, *Int. J. Archit. Herit.* **8**:3 (2014), 312–335.
- [Block and Lachauer 2014b] P. Block and L. Lachauer, “Three-dimensional funicular analysis of masonry vaults”, *Mech. Res. Commun.* **56** (2014), 53–60.
- [Block and Ochsendorf 2007] P. Block and J. Ochsendorf, “Thrust network analysis: a new methodology for three-dimensional equilibrium”, *J. IASS* **48**:3 (2007), 167–173.
- [Block and Ochsendorf 2008] P. Block and J. Ochsendorf, “Lower-bound analysis of masonry vaults”, pp. 593–600 in *Structural analysis of historic construction: preserving safety and significance* (Bath, UK, 2008), edited by D. D’Ayala and E. Fodde, Proc. Int. Conf. Struct. Anal. Historic Constr. **6**, CRC, London, 2008.
- [Brocato 2011] M. Brocato, “Reciprocal frames: kinematical determinacy and limit analysis”, *Int. J. Space Struct.* **26**:4 (2011), 343–358.
- [Brocato 2018] M. Brocato, “A continuum model of interlocking structural systems”, *Rend. Accad. Naz. Lincei* **29**:1 (2018), 63–83.
- [Brocato and Mondardini 2010] M. Brocato and L. Mondardini, “Geometric methods and computational mechanics for the design of stone domes based on Abeille’s bond”, pp. 149–162 in *Advances in architectural geometry* (Vienna, 2010), edited by C. Ceccato et al., Springer, 2010.
- [Brocato and Mondardini 2012] M. Brocato and L. Mondardini, “A new type of stone dome based on Abeille’s bond”, *Int. J. Solids Struct.* **49**:13 (2012), 1786–1801.
- [Brocato and Mondardini 2015] M. Brocato and L. Mondardini, “Parametric analysis of structures from flat vaults to reciprocal grids”, *Int. J. Solids Struct.* **54** (2015), 50–65.

- [Brocato et al. 2014] M. Brocato, W. Deleporte, L. Mondardini, and J.-E. Tanguy, “A proposal for a new type of prefabricated stone wall”, *Int. J. Space Struct.* **29**:2 (2014), 97–112.
- [Ciblac and Fantin 2015] T. Ciblac and M. Fantin, “Rediscovering Durand-Claye’s method using force network method implemented for construction history”, pp. 439–446 in *Proc. Fifth International Congress on Construction History* (Chicago, 2015), edited by D. Friedman et al., Constr. Hist. Soc. Amer., Chicago, 2015.
- [Dyskin et al. 2001] A. V. Dyskin, Y. Estrin, A. J. Kanel-Belov, and E. Pasternak, “A new concept in design of materials and structures: assemblies of interlocked tetrahedron-shaped elements”, *Scr. Mater.* **44**:12 (2001), 2689–2694.
- [Dyskin et al. 2003a] A. V. Dyskin, Y. Estrin, A. J. Kanel-Belov, and E. Pasternak, “A new principle in design of composite materials: reinforcement by interlocked elements”, *Compos. Sci. Technol.* **63**:3-4 (2003), 483–491.
- [Dyskin et al. 2003b] A. V. Dyskin, Y. Estrin, A. J. Kanel-Belov, and E. Pasternak, “Topological interlocking of platonic solids: a way to new materials and structures”, *Philos. Mag. Lett.* **83**:3 (2003), 197–203.
- [Émy 1837] A.-R. Émy, *Traité de l’art de la charpenterie*, Carilian-Gœury, Paris, 1837.
- [Estrin et al. 2004] Y. Estrin, A. V. Dyskin, E. Pasternak, S. Schaare, S. Stanchits, and A. J. Kanel-Belov, “Negative stiffness of a layer with topologically interlocked elements”, *Scr. Mater.* **50**:2 (2004), 291–294.
- [Estrin et al. 2011] Y. Estrin, A. V. Dyskin, and E. Pasternak, “Topological interlocking as a material design concept”, *Mater. Sci. Eng. C* **31**:6 (2011), 1189–1194.
- [Etlin et al. 2008] R. A. Etlin, G. Fallacara, and L. C. P. Tamborero, *Plaited stereotomy: stone vaults for the modern world*, Aracne, Rome, 2008.
- [Fallacara 2006] G. Fallacara, “Digital stereotomy and topological transformations: reasoning about shape building”, pp. 1075–1092 in *Proc. Second International Congress on Construction History, I* (Cambridge, 2006), edited by M. Dunkeld et al., Constr. Hist. Soc., Cambridge, 2006.
- [Fallacara 2009] G. Fallacara, “Toward a stereotomic design: experimental constructions and didactic experiences”, pp. 553–559 in *Proc. Third International Congress on Construction History* (Cottbus, Germany, 2009), edited by K.-E. Kurrer et al., Neunplus1, Berlin, 2009.
- [Fantin 2017] M. Fantin, *Étude des rapports entre stéréotomie et résistance des voûtes clavées*, Ph.D. thesis, Université Paris-Est, 2017, <http://tel.archives-ouvertes.fr/tel-01834617>.
- [Fantin and Ciblac 2016] M. Fantin and T. Ciblac, “Extension of thrust network analysis with joints consideration and new equilibrium states”, *Int. J. Space Struct.* **31**:2-4 (2016), 190–202.
- [Fleury 2009] F. Fleury, “Evaluation of the perpendicular flat vault inventor’s intuitions through large scale instrumented testing”, pp. 611–618 in *Proc. Third International Congress on Construction History* (Cottbus, Germany, 2009), edited by K.-E. Kurrer et al., Neunplus1, Berlin, 2009.
- [Fleury 2010] F. Fleury, “Les idées sous-jacentes à la conception de la voûte plate perpendiculaire”, pp. 283–291 in *Édifices & artifices: histoires constructives* (Paris, 2008), edited by R. Carvais et al., Picard, Paris, 2010.
- [Fraternali 2010] F. Fraternali, “A thrust network approach to the equilibrium problem of unreinforced masonry vaults via polyhedral stress functions”, *Mech. Res. Commun.* **37**:2 (2010), 198–204.
- [Frézier 1738] A.-F. Frézier, *La théorie et la pratique de la coupe des pierres et des bois pour la construction des voûtes et autres parties des bâtiments civils et militaires, ou traité de stereotomie a l’usage de l’architecture, II*, Doulsseker, Strasbourg, 1738.
- [Gallon 1735] J.-G. Gallon, *Machines et inventions approuvées par l’Académie royale des sciences, depuis son établissement jusqu’à présent, avec leur description, I*, Martin, Coignard, Guerin, Paris, 1735.
- [de Goes et al. 2013] F. de Goes, P. Alliez, H. Owahdi, and M. Desbrun, “On the equilibrium of simplicial masonry structures”, *ACM Trans. Graph.* **32**:4 (2013), art. id. 93.
- [Heyman 1995] J. Heyman, *The stone skeleton: structural engineering of masonry architecture*, Cambridge Univ. Press, 1995.
- [Khandelwal et al. 2012] S. Khandelwal, T. Siegmund, R. J. Cipra, and J. S. Bolton, “Transverse loading of cellular topologically interlocked materials”, *Int. J. Solids Struct.* **49**:18 (2012), 2394–2403.
- [Khandelwal et al. 2015] S. Khandelwal, T. Siegmund, R. J. Cipra, and J. S. Bolton, “Adaptive mechanical properties of topologically interlocking material systems”, *Smart Mater. Struct.* **24**:4 (2015), art. id. 045037.

- [López Mozo 2003] A. López Mozo, “Planar vaults in the Monastery of El Escorial”, pp. 1327–1334 in *Proc. First International Congress on Construction History* (Madrid, 2003), edited by S. Huerta Fernández, Inst. Juan de Herrera, Madrid, 2003.
- [Mondardini 2015] M. L. Mondardini, *Contribution au développement des structures en pierre de taille: modélisation, optimisation et outils de conception*, Ph.D. thesis, Université Paris-Est, 2015, <https://tinyurl.com/mond2015>.
- [de Nichilo 2003] E. de Nichilo, “Learning from stone traditional vaulted systems for the contemporary project of architecture”, pp. 743–754 in *Proc. First International Congress on Construction History, II* (Madrid, 2003), edited by S. Huerta Fernández, Inst. Juan de Herrera, Madrid, 2003.
- [O’Dwyer 1999] D. O’Dwyer, “Funicular analysis of masonry vaults”, *Comput. Struct.* **73**:1-5 (1999), 187–197.
- [Pérouse de Montclos 1982] J.-M. Pérouse de Montclos, *L’architecture à la française: du milieu du XVe à la fin du XVIIIe siècle*, Picard, Paris, 1982.
- [Rabasa Díaz 1998] E. Rabasa Díaz, “La bóveda plana de Abeille en Lugo”, pp. 409–415 in *Actas del Segundo Congreso Nacional de Historia de la Construcción* (A Coruña, Spain, 1998), edited by F. Bores et al., Inst. Juan de Herrera, Madrid, 1998.
- [Rabasa Díaz and López Mozo 2012] E. Rabasa Díaz and A. López Mozo, “Les joints occultes sur plates-bandes et voûtes plates en Espagne”, pp. 288–295 in *L’architrave, le plancher, la plate forme: Nouvelle histoire de la construction*, edited by R. Gargiani, Presses Polytech. Univ. Romandes, Lausanne, Switzerland, 2012.
- [Rippmann et al. 2012] M. Rippmann, L. Lachauer, and P. Block, “Interactive vault design”, *Int. J. Space Struct.* **27**:4 (2012), 219–230.
- [Rondelet 1804] J. Rondelet, *Traité théorique et pratique de l’art de bâtir*, tome II, Chez l’Auteur, Paris, 1804.
- [Rondelet 1828] J. Rondelet, *Traité théorique et pratique de l’art de bâtir: planches*, Chez l’Auteur, Paris, 1828.
- [Sakarovitch 2006] J. Sakarovitch, “Construction history and experimentation”, pp. 2777–2792 in *Proc. Second International Congress on Construction History* (Cambridge, 2006), edited by M. Dunkeld, Constr. Hist. Soc., Cambridge, 2006.
- [van Swinderen and Coenders 2009] T. van Swinderen and J. Coenders, “Tool to design masonry double-curved shells”, pp. 1136–1144 in *Evolution and trends in design, analysis and construction of shell and spatial structures* (Valencia, 2009), edited by A. Domingo and C. Lázaro, Editorial UPV, Valencia, 2009.
- [Uva 2003] G. R. Uva, “Learning from traditional vaulted systems for the contemporary design: an updated reuse of flat vaults: analysis of structural performance and recent safety requirements”, pp. 2015–2021 in *Proc. First International Congress on Construction History* (Madrid, 2003), edited by S. Huerta Fernández, Inst. Juan de Herrera, Madrid, 2003.
- [Vouga et al. 2012] E. Vouga, M. Höbinger, J. Wallner, and H. Pottmann, “Design of self-supporting surfaces”, *ACM Trans. Graph.* **31**:4 (2012), art. id. 87.
- [Weizmann et al. 2016] M. Weizmann, O. Amir, and Y. J. Grobman, “Topological interlocking in buildings: a case for the design and construction of floors”, *Automation Constr.* **72**:1 (2016), 18–25.
- [Yeomans 1997] D. Yeomans, “The Serlio floor and its derivations”, *Archit. Res. Quart.* **2**:3 (1997), 74–83.

Received 16 Jun 2018. Revised 28 Jan 2019. Accepted 4 Feb 2019.

MATHIAS FANTIN: mathias.fantin@polytechnique.edu
Laboratoire GSA, ENSA Paris-Malaquais, Paris, France

THIERRY CIBLAC: thierry.ciblac@paris-malaquais.archi.fr
Laboratoire GSA, ENSA Paris-Malaquais, Paris, France

MAURIZIO BROCATO: maurizio.brocato@paris-malaquais.archi.fr
Laboratoire GSA, ENSA Paris-Malaquais, Paris, France

JOURNAL OF MECHANICS OF MATERIALS AND STRUCTURES

msp.org/jomms

Founded by Charles R. Steele and Marie-Louise Steele

EDITORIAL BOARD

ADAIR R. AGUIAR	University of São Paulo at São Carlos, Brazil
KATIA BERTOLDI	Harvard University, USA
DAVIDE BIGONI	University of Trento, Italy
MAENGHYO CHO	Seoul National University, Korea
HUILING DUAN	Beijing University
YIBIN FU	Keele University, UK
IWONA JASIUK	University of Illinois at Urbana-Champaign, USA
DENNIS KOCHMANN	ETH Zurich
MITSUTOSHI KURODA	Yamagata University, Japan
CHEE W. LIM	City University of Hong Kong
ZISHUN LIU	Xi'an Jiaotong University, China
THOMAS J. PENCE	Michigan State University, USA
GIANNI ROYER-CARFAGNI	Università degli studi di Parma, Italy
DAVID STEIGMANN	University of California at Berkeley, USA
PAUL STEINMANN	Friedrich-Alexander-Universität Erlangen-Nürnberg, Germany
KENJIRO TERADA	Tohoku University, Japan

ADVISORY BOARD

J. P. CARTER	University of Sydney, Australia
D. H. HODGES	Georgia Institute of Technology, USA
J. HUTCHINSON	Harvard University, USA
D. PAMPLONA	Universidade Católica do Rio de Janeiro, Brazil
M. B. RUBIN	Technion, Haifa, Israel

PRODUCTION production@msp.org

SILVIO LEVY Scientific Editor


Cover photo: Wikimedia Commons

See msp.org/jomms for submission guidelines.

JoMMS (ISSN 1559-3959) at Mathematical Sciences Publishers, 798 Evans Hall #6840, c/o University of California, Berkeley, CA 94720-3840, is published in 10 issues a year. The subscription price for 2018 is US \$615/year for the electronic version, and \$775/year (+\$60, if shipping outside the US) for print and electronic. Subscriptions, requests for back issues, and changes of address should be sent to MSP.

JoMMS peer-review and production is managed by EditFLOW® from Mathematical Sciences Publishers.

PUBLISHED BY

 **mathematical sciences publishers**
nonprofit scientific publishing

<http://msp.org/>

© 2018 Mathematical Sciences Publishers

**Special issue on
Structural Analysis
of Real Historic Buildings (part 1)**

Preface	MAURIZIO ANGELILLO and SANTIAGO HUERTA FERNÁNDEZ	607
The structural engineer's view of ancient buildings	JACQUES HEYMAN	609
Mechanics of flying buttresses: the case of the cathedral of Mallorca	PAULA FUENTES	617
Analysis of 3D no-tension masonry-like walls	DEBORAH BRICCOLA, MATTEO BRUGGI and ALBERTO TALIERCIO	631
Cracking of masonry arches with great deformations: a new equilibrium approach	JOSÉ IGNACIO HERNANDO GARCÍA, FERNANDO MAGDALENA LAYOS and ANTONIO AZNAR LÓPEZ	647
Resistance of flat vaults taking their stereotomy into account	MATHIAS FANTIN, THIERRY CIBLAC and MAURIZIO BROCATO	657
Seismic vulnerability of domes: a case study	CONCETTA CUSANO, CLAUDIA CENNAMO and MAURIZIO ANGELILLO	679
Orthotropic plane bodies with bounded tensile and compressive strength	MASSIMILIANO LUCCHESI, BARBARA PINTUCCHI and NICOLA ZANI	691
A no-tension analysis for a brick masonry vault with lunette	MICHELA MONACO, IMMACOLATA BERGAMASCO and MICHELE BETTI	703